*Physical Modelling in Geotechnics*


# Centrifuge apparatus for modelling helical anchor response under snatch loads

P.Y. Duverneuil, C. Gaudin, B. Bienen, F. Bransby & H. Mohr
*University of Western Australia, Perth, Australia*
*Marine Energy Research Australia, Albany, Australia*

**ABSTRACT:** Helical anchors have potential to provide the offshore industry with an economically competitive method to found renewable infrastructure. For offshore floating devices, snatch events can occur when a slack tether of the buoyant body becomes suddenly taut. Estimation of the capacity of the anchor during these dynamic events is needed to ensure reliable geotechnical design. This paper presents a pioneering experimental investigation into the soil deformation around shallow embedded helical anchors under snatch events using high-speed Particle Image Velocimetry (PIV) measurements in the centrifuge environment. Preliminary findings help to understand the additional capacity of the foundation system observed under dynamic loading.

**Keywords:** helical anchors, centrifuge modelling, snatch loading, Particle Image Velocimetry (PIV).

## 1 INTRODUCTION

Helical anchors are composed of one or multiple helical plates welded to a central shaft. They have extensively been studied and used for onshore applications and are suggested as an alternative solution to anchor offshore energy floating bodies, providing high tensile and compressive capacities due to the helix and generating minimal noise during installation.

Recent research has focused on anchor response under quasi-static tension or compression loads (e.g. Hao et al., 2019, Lutenegger and Tsuha, 2015), their behaviour during installation (Cerfontaine et al., 2021a, 2021b) and their behaviour under in-service loading conditions offshore. The latter has focused primarily on the quasi-static cyclic response of anchors (Schiavon et al., 2019). However, floating bodies can also experience significant dynamic events when a slack mooring line becomes suddenly taut (Davidson and Ringwood, 2017). These specific loadings, responsible for the highest load magnitudes on the foundation in a short period of time, are known as 'snatch' loads. Under snatch loads in dry sand, additional capacity is observed, associated with the inertia of the anchor and mobilised soil mass (Duong, 2019). As a consequence, estimating the anchor capacity under dynamic loads depends on accurate estimations of the failure mechanism and thereby the accelerated soil mass.

This paper describes novel experimental apparatus used to capture the response of large helical anchors under snatch loads. The centrifuge set-up allows the investigation of the additional resistance due to inertial effects by Particle Image Velocimetry (PIV) techniques, which can reveal the continuous deformation of the soil and its progressive failure.

## 2 Experimental details

### 2.1 Test set-up

The experiments presented in this paper were conducted in the 3.6 m diameter centrifuge at the National Geotechnical Centrifuge Facility (Randolph et al., 1991) at an acceleration level of 60g. The set-up described here includes a PIV box, a dual actuator loading apparatus and a high-speed acquisition system.

An overview of the PIV box with anchor models is presented in Fig. 1. The set-up allows the anchor models to be pre-embedded in dry sand and up to four separate tests to be conducted in a single box. The assembly includes a PIV box (inner dimensions 335 x 225 x 300 mm) with Perspex windows, modular anchors built from four components (inner shaft, tubes, circular plate and a top cap) and a guiding system (base and top guides) to keep the anchor against the window throughout the test. A thin layer of urethane compound was moulded on the edge of the anchor to prevent scratches on the window and to reduce frictional resistance. A foam layer was installed in the base to allow settlement of the anchor during ramp-up of the centrifuge, thereby minimising the likelihood of the anchor being subjected to positive or negative vertical soil loading before the uplift event.

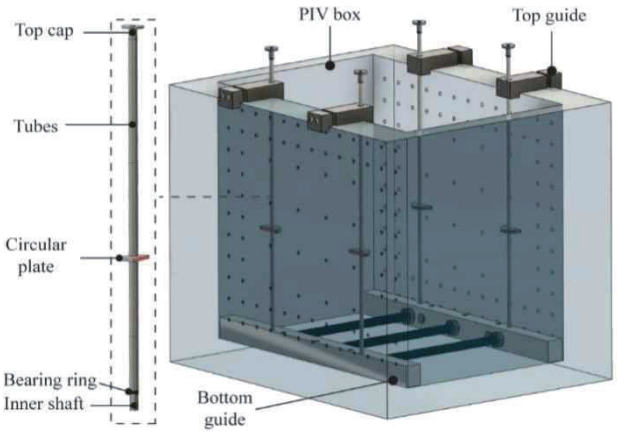


Fig. 1. PIV box with modular anchor and guiding components.

An anchor plate with diameter $D$ of 27 mm (1.6 m in prototype scale) representative of a large anchor helix suitable for offshore use was embedded to a depth $L$ of 120 mm ($L/D$ = 4.5). The single-helix anchor geometry was simplified to a flat semi-circular plate to isolate the snatch loading performance from installation effects.

This PIV box was housed in a larger strongbox, supporting the snatch loading apparatus (Duong, 2019) which was adapted to perform dynamic loading in a more confined space (see Fig. 2a). To perform the dynamic loading, a dual actuator system was used. The first actuator was raised and held a mass with a paddle. The mass was connected to the anchor with a wire, passing through a pulley system supported by the second actuator. The first actuator movement pulled the supporting paddle out allowing the mass to free fall in the enhanced gravity environment, generating a short impulse load of high magnitude on the anchor. Varying the dropping height allowed the distance travelled by the mass to be increased or decreased, thereby changing the resultant maximal velocity and the momentum transferred by the wire to the anchor. The anchor cap and the masses were instrumented with micro-electromechanical systems (MEMS) accelerometers, to allow acceleration, velocity and displacement of the mass and anchor to be monitored. A linear variable displacement transducer (LVDT) (as a backup) and a load cell were mounted on the anchor cap. Data was recorded at a sampling frequency of 50 kHz.

To capture the continuous deformation of the soil under dynamic loading, a high-speed camera (MotionBLITZ Cube) manufactured by Mikrotron, was secured on a support in the strong box (Fig. 2b). Although the camera was able to record up to 45 000 frames at low resolution, the success of PIV techniques depends on a high resolution acquisition of images in the soil domain. Consequently, the field of view was reduced to half of the region around the anchor plate to allow axisymmetric analysis of the image (Fig. 2c). The image acquisition rate was set to 2230 frames per second. Three LED light panels were necessary to provide sufficient and even lighting.

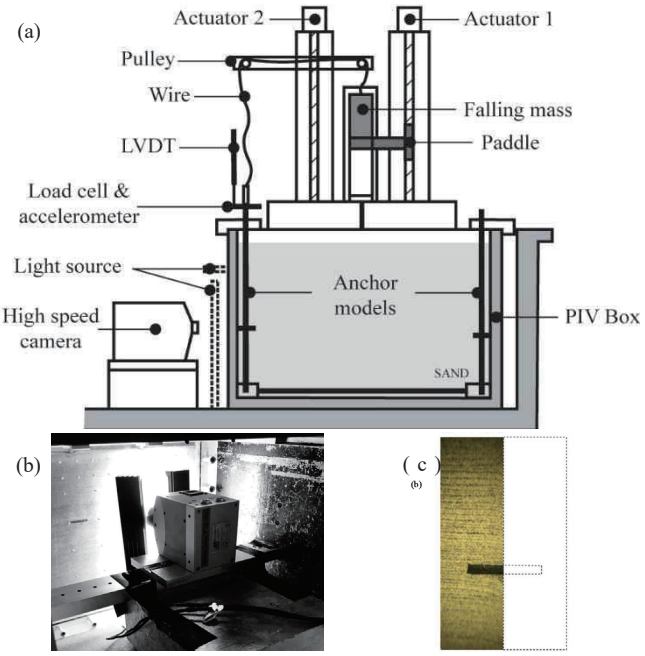


Fig. 2. (a) Schematic illustration of the set-up (b) High-speed camera (c) Axisymmetric field of view.

## 2.2 Sample preparation and sample characterisation

The tests were conducted in dry superfine University of Western Australia (UWA) silica sand, with properties summarised by Chow et al. (2019). Artificial 'texture' was added to increase the visual contrast between sand particles, with a fraction of sand grains dyed black, without modifying the soil element properties. The ratio between the anchor plate radius to the median sand grain size ($R/d_{50}$) was 74, allowing grain scale effects to be considered negligible.

The sample was prepared by sand pluviation. The test was designed as 'wished-in-place' to avoid installation effects and ensure consistency between tests. A gradual setting-up of the anchor during the pluviation process allowed local sand density variations under the plate due to shadowing effect to be avoided: once the sample height reached the targeted plate embedment $L$, pluviation was paused to install the plate on the sand layer, before pluviation was continued to reach the full embedment. After pluviation, the sample was spun up and down to the desired acceleration level to avoid further densification during the test campaign. From weight and volume measurements, the relative density was confirmed to be around 66%.

Sample characterisation was carried out prior to the dynamic testing by two cone penetrometer tests (CPTs) using a 5 mm diameter cone, which confirmed the uniformity across the sample.

### 2.3 Testing procedure

The testing procedure is described in Fig. 3, with the evolution of (a) acceleration, (b) velocity, and (c) displacement recorded for the mass (dashed line) and anchor (continuous line), and (d) axial load with time. The test sequence is divided into four stages: (i) the mass is released by the actuator and accelerates until reaching the g-field level and its velocity increases linearly until the wire becomes taut and the momentum is transferred to the anchor; (ii) the anchor is loaded, its velocity and its acceleration increase and the mass decelerates; (iii) at this point, the peak force is mobilised, and the mass oscillates vertically, (iv) until the system regains static equilibrium where a residual load is applied due to the (static) mass hanging on the wire. During the specific test presented in Fig. 3, the anchor reached a maximal acceleration of 137 g, and a velocity of 2.1 m/s.

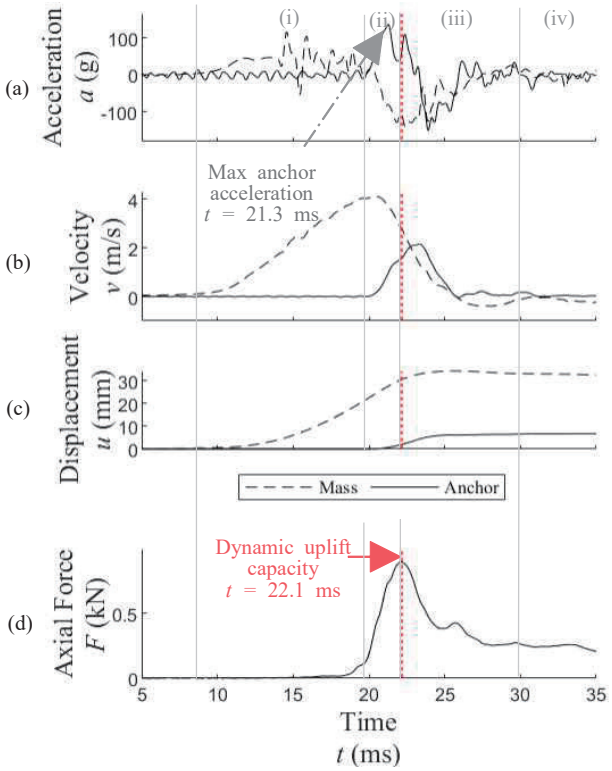


Fig. 3. Time series of dynamic uplift event in dry sand.

## 3 PIV ANALYSIS

GeoPIV-RG (Stanier et al., 2016a) was used to measure soil deformations and failure mechanisms at the anchor depth from the captured images. The automatic reference image updated scheme was selected to allow measurements of large deformations, subset appearance changes or grain rearrangement maximising correlations between successive measurements, as recommended by Stanier et al. (2016b). Lens deflection was estimated to be negligible by chessboard calibration correction prior to the testing, allowing a linear scaling of the recorded image.

## 4 Initial RESULTS AND DISCUSSION

### 4.1 Load displacement response

A comparison of the dynamic load-displacement behavior of the anchor with a quasi-static uplift test is shown in Fig. 4. The displacement $u$ is normalised by the plate diameter, and the axial force $F$ is normalised by the unit weight $\gamma$, the square of the anchor diameter and the embedment. The quasi-static response is typical of that expected for dense sand (Ilamparuthi et al, 2002) with a considerable number of load oscillations initially associated with the collapse of sand particles in the gap created underneath the anchor plate. The axial capacity of the dynamic test is observed to be 25% higher than the quasi-static capacity, while the displacement to achieve the peak load is reduced to 30% of the quasi static displacement. Fig. 4 also indicates the image acquisition data points. A reasonable number of images were recorded before the anchor reached its dynamic capacity, thereby allowing mechanisms to be observed.

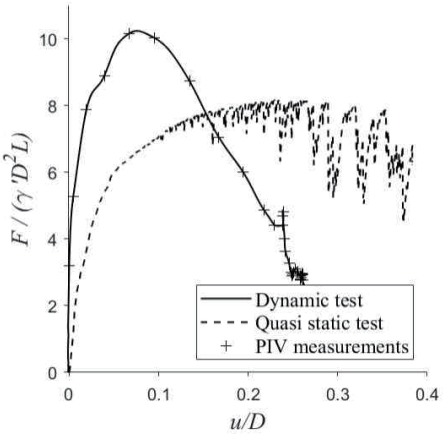


Fig. 4. Load-displacement response of the foundation to quasi-static and dynamic loading rates.

### 4.2 Displacement and acceleration fields

Knowledge of the displacement and acceleration fields help to understand the different contributions to the foundation resistance under snatch load. The absolute displacement field at failure for the dynamic test is shown in Fig. 5a. Even though the field of observation is limited in depth, a conical failure pattern extending to the soil surface is observed, with the development of shear resistance along inclined slip lanes similar to that observed for quasi-static responses of shallow embedded anchors (Liu et al., 2012). Additionally, in order to quantify the inertial component of the dynamic resistance, a reliable estimation of the acceleration field throughout the test must be made. The resultant acceleration contours are plotted on Fig. 5b

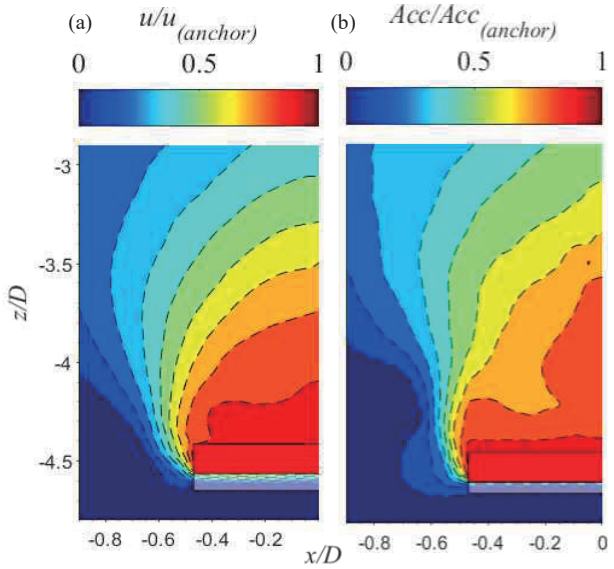


Fig. 5. Results of PIV analysis: (a) displacement contours at peak load and (b) acceleration contours at maximal acceleration.

for the maximal acceleration (at t = 21.3 ms), which occurs before the peak uplift resistance is reached. An acceleration zone of magnitude equal to the anchor acceleration is localised above the shallow embedded anchor. At a depth of three plate diameters (top limit of the field of view), the maximal acceleration of the sand particles is reduced to half of the anchor acceleration. The non-uniformity of the acceleration field indicates soil compression and volume change which eventually helps to understand the distribution of the maximal inertial component of the dynamic resistance with depth. Although additional investigation is needed, this observation paves the way for successful estimation of the contribution of the inertial component to the resistance under dynamic uplift loading.

## 5 CONCLUSION

This paper has detailed the development of novel centrifuge apparatus that allows investigation of soil response around a single-helix anchor under dynamic snatch loads. The apparatus makes it possible to investigate the response of foundations under different loading rates, while capturing the soil deformation at the anchor depth with a high-speed camera.

Quasi-static and dynamic responses were compared. Dynamic loading of the anchor plate results in additional resistance due to the inertia of the anchor and soil mass. The high-speed PIV measurements allow accurate estimation of the displacement field around the plate to observe the corresponding failure mechanisms, and estimation of the associated acceleration field. The latter provides evidence of an inertial component contribution to the foundation uplift resistance localised in an area above the anchor plate.

## ACKNOWLEDGEMENTS

This research was conducted by Marine Energy Research Australia and jointly funded by UWA and the Western Australian Government, via the Department of Primary Industries and Regional Development (DPIRD). The authors acknowledge the Australia- China Science and Research Fund, Australian Department of Industry, Innovation and Science. The fourth author holds the Fugro Chair, whose support is gratefully acknowledged.

## REFERENCES

Cerfontaine, B., Brown, M., Knappett, J., Davidson, C., Sharif, Y., Huisman, M., Ottolini, M., & Ball, J. D. 2021a. Control of screw pile installation to optimise performance for offshore energy applications. *Géotechnique*.

Cerfontaine, B., Ciantia, M., Brown, M. J., & Sharif, Y. U. 2021b. DEM study of particle scale and penetration rate on the installation mechanisms of screw piles in sand. *Computers and Geotechnics* 139: 104380.

Chow, S. H., Roy, A., Herduin, M., Heins, E., King, L., Bienen, B., O'Loughlin, C., Gaudin, C., & Cassidy, M. 2019. Characterisation of UWA superfine silica sand.

Davidson, J., & Ringwood, J. 2017. Mathematical Modelling of Mooring Systems for Wave Energy Converters - A Review. *Energies* 10(5)

Duong, M.-T. 2019. An investigation into the performance of anchors under dynamic loading. PhD thesis, UWA.

Hao, D., Wang, D., O'Loughlin, C. D., & Gaudin, C. 2019. Tensile monotonic capacity of helical anchors in sand: interaction between helices. *Canadian Geotechnical Journal* 56(10):1534-1543.

Ilamparuthi, K., Dickin, E. A., & Muthukrisnaiah, K. 2002. Experimental investigation of the uplift behaviour of circular plate anchors embedded in sand. *Canadian Geotechnical Journal* 39(3): 648-664.

Liu, J., Liu, M., and Zhu, Z. 2012. Sand deformation around an uplift plate anchor. *Journal of Geotechnical and Geoenvironmental Engineering* 138 (6): 728-737.

Lutenegger, A. J., & Tsuha, C. D. H. 2015. Evaluating installation disturbance from helical piles and anchors using compression and tension tests. *Proc. of the 15th Pan-American Conf. on Soil Mechanics and Geotechnical Engineering:* 373-381.

Randolph, M. F., Jewell, R. J., Stone, K. J. L., & Brown, T. A. 1991. Establishing a new centrifuge facility. *Proc. Int. Conf. Centrifuge 9.* Rotterdam, the Netherlands: A.A. Balkem.

Schiavon, J. A., Tsuha, C. D. H. C., Neel, A., & Thorel, L. 2019. Centrifuge modelling of a helical anchor under different cyclic loading conditions in sand. *Int. Journal of Physical Modelling in Geotechnics* 19(2): 72-88.

Stanier, S., Blaber, J., Take, W. A., & White, D. J. 2016a. Improved image-based deformation measurement for geotechnical applications. *Canadian Geotechnical Journal* 53(5): 727-739.

Stanier, S., Dijkstra, J., Leśniewska, D., Hambleton, J., White, D., & Muir Wood, D. 2016b. Vermiculate artefacts in image analysis of granular materials. *Computers and Geotechnics* 72: 100-113.